Profile Control of Patterned Plasma Deposition and Etching

J. Wang[1], P. Bulkin[1], P. Roca i Cabarrocas[1], K. Ouaras[1], S. Filonovich[2], and E.V. Johnson[1]

[1] *LPICM, CNRS, Ecole polytechnique, Instut Polytechnique de Paris, Palaiseau, France*
[2] *TotalEnergies, OneTech, 2 Place Jean Millier, 92400, Courbevoie, France*

Abstract: The use of a patterned electrode in a plasma-enhanced chemical vapour deposition system allows one to perform deposition or etching in a pattern without resorting to masking or lithography. However, the profile of the etched area can be critical for some applications, such as interdigitated solar cells. Said profile depends strongly on the process conditions and gas chemistry of the plasma that lights within the slits of the patterned electrode. We show some typical profiles that originate from such deposition processes, and how changes to the gas mixture can tailor the profile.

Keywords: Patterned deposition, etching

1. Introduction

Recent work has demonstrated how the use of a patterned electrode in a capacitively coupled plasma system allows one to perform patterned deposition or etching of semiconductor thin films [1][2]. By placing the radio-frequency (RF) electrode in close proximity (~200 µm) to the substrate, the plasma can only light in the areas where slits are present in the electrode (as shown in Figure 1). The plasma is therefore localized within the slit, and the plasma process to the area underneath it.

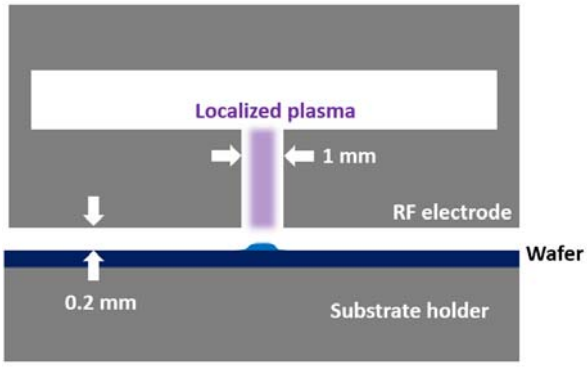

Figure 1. Representation of plasma localization obtained by adding a 1mm wide slit in the RF electrode. The deposition resulting from the plasma is localized to an area under the slit.

However, the localization of the process is not a perfect mapping of the slit, as the growth or etching precursors will diffuse or drift from their point of origin to the surface, creating a profile on the surface. This profile can be of increased importance for certain applications, as shown in figure 2. In this figure, an interdigitated back contact (IBC) solar cell structure is shown, with two different etching profiles. In this architecture, the P and N contacts are limited to areas where the complete stack is present. For the less abrupt profile, one can see that the spacing between the N and P contacts (red arrow) is significant, whereas a more abrupt profile allows the contact to be much more closely spaced (green arrows). This means that photocarriers have to diffuse a lesser distance, increasing the likelihood of their collection.

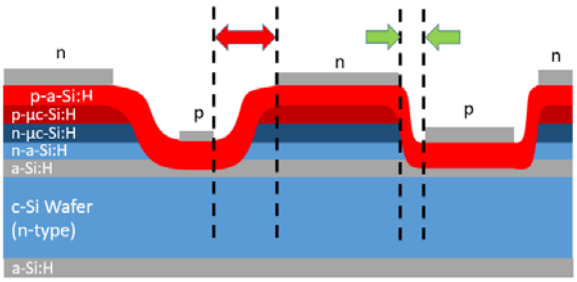

Figure 2. Representation of importance of etched profile for IBC solar cell application. The proximity of the P and N contacts is governed by the abruptness of the profile.

2. Experiment setup

The experiments have been performed in a custom made RF CCP reactor. The electrodes are aluminium for the deposition experiments, and stainless steel for the etching experiments. The slits in the electrode are 1 mm across, and the interelectrode distance in the non-plasma areas is ~0.2mm. Process pressures were between 6 and 10 Torr. The deposition experiments were done using a mixture of SiH_4, H_2, and Ar, and with the substrate holder and electrode at a temperature of 200°C. Most of the etching experiments have be done using mixtures of NF_3, Ar and N_2, and were performed at room temperature. The etching experiments have also been done using a pulsed plasma to slow down the etching, which is very rapid due to the hollow cathode effect within the slits [3][4]. Profilometry measurements were performed using a Dektak XT (Bruker), and in once case, were confirmed by spectroscopic ellipsometry (Horiba UVISEL 2).

3. Results and Discussion

Deposition results- A typical profile for hydrogenated amorphous silicon (a-Si:H) deposition from SiH_4, H_2, and Ar is shown in figure 3 (same data as from [1]). One first notes that the deposition profile is narrower that that of the slit. The width of the profile is 750 µm at its base, narrower than the 1 mm slit. Moreover, it is not a perfectly rectangular profile (the width at the top is about 500µm).

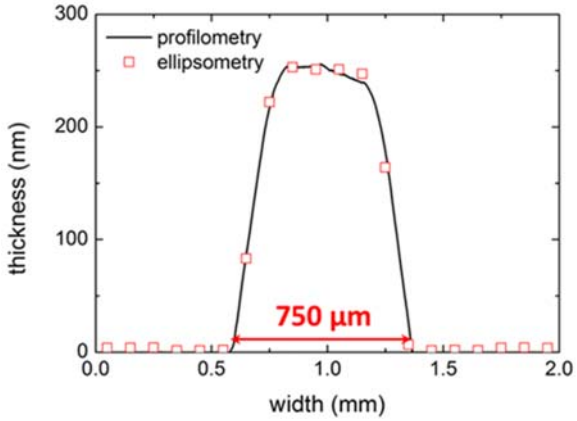

Figure 3. Profile of deposited a-Si:H strip using a 1 mm wide trench.

A second example of the profile of a deposited a-Si:H strip is shown in Figure 4, this time for a set of three slits (same data as [2]). The gas mixture in this case was leaner (less SiH_4) than the case of Figure 3, but still produced an a-Si:H film. One notes different features in this profile, notably the presence of two trenches beside each one of the deposition peaks. In fact, as discussed in [2], these profiles are the result of competing deposition and etching process, as the H radicals produced are effective a-Si:H etchants. By superimposing a narrow deposition profile and a broader profile for etching, one can produce the profiles of fig. 4.

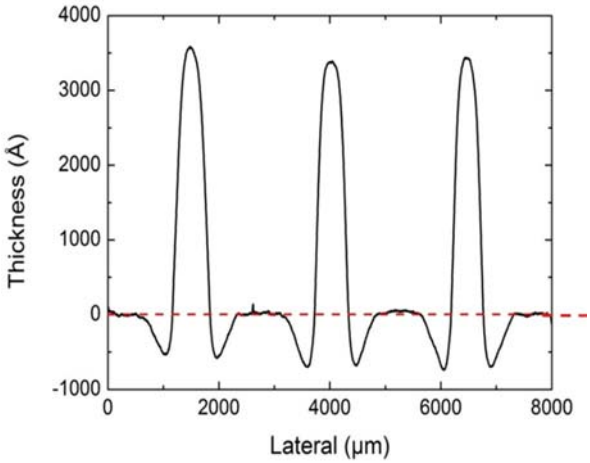

Figure 4. Profile of a series of a-Si:H strips deposited under leaner SiH_4 conditions. Notice appearance of etched trenches beside the deposited strip.

Etching results – A typical profile for an etched trench using the NF_3/Ar gas mixture is presented in Figure 5. Notice, in this case, that although the FWHM of the trench is narrower than the slit (800µm vs 1000 µm), the width of the profile at the base is much greater than that of the slit. As well, one can note the presence of two superimposed, inverted peaks in this profile, each with different widths (as was the case in Figure 4, but for a deposition "peak" and an inverted "etching" peak).

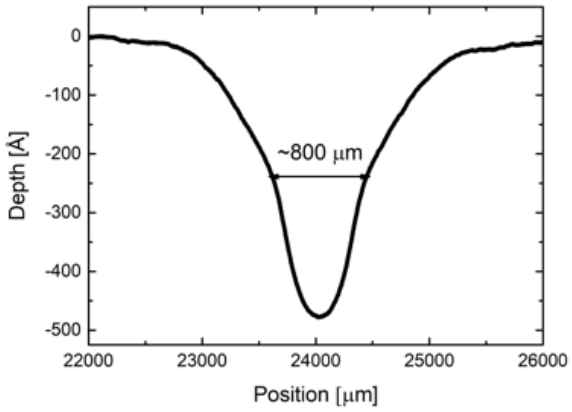

Figure 5. Profile of etched trench using 1mm wide slit and NF_3+Ar gas mixture.

By changing the gas mixture, one can modulate the contribution and width of these two peaks, as presented in Figure 6. By tuning the NF_3, Ar, and N_2 gas mixture, one can select a narrower profile, and even produce a "Bactrian Camel hump" effect (black curve of Figure 6), with two bumps appearing around the central peak.

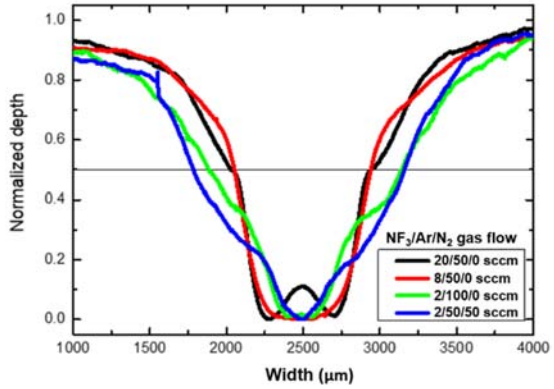

Figure 6. Series of profiles of etched trenches using various gas mixtures of NF_3, Ar, and N_2, all using the same slit width and spacing.

The double bump of the black curve in Figure 6 (for 20/50 NF_3/Ar) is reminiscent of the appearance of microtrenching in microelectronics etching [5][6], but in this case, are appearing at length scales that are more than 1000 times greater.

The etched and deposition profiles that manifest themselves when using a patterned electrode to perform maskless processing can be influenced by a number of factors. Firstly, and one that has been controlled in the

above work is the interelectrode distance. If the substrate is not placed sufficiently close to the electrode, then the profile will become much broader than the slit, and in the extreme case, is not longer patterned on the substrate. In this case, the electrode functions more like a multi-hollow cathode, producing a more intense plasma, but a uniform one [7]. This effect has been controlled in the above work by keeping the interelectrode distance very small.

Beyond this effect, many further mechanisms will affect the profile: (1) where the etching and/or growth precursors are generated within the slit, (2) the distance over which they can travel (before being consumed by the wall or by gas phase reactions), and (3) the ion distribution profile on the surface for ion-assisted processes. For processes limited by the contribution of radicals, these first two points will be the most important. It is reasonable that the two peaks of different widths are caused by radical generation at the top and bottom of the slit during the sheath expansions. On the other hand, one must carefully consider the direct role of ions in the growth processes. Previous work has shown that under specific, high pressure and hydrogen-rich conditions, silicon-containing ions can contribute an appreciable amount to amorphous and microcrystalline silicon film growth [8]. Indeed, simulation using a simple Ar plasma showed many similar features to the deposition profile [1], although a much richer variety of profiles has since been observed.

Explaing the double "camel" peaks is not as straightforward. The "microtrenching" observed in microelectronics etching is explained either by the charging of dielectric sidewalls deflecting positive ions, or sidewall passivation reflecting neutrals. However, it is not evident how the same processes could be occurring in this work; the sidewalls of the trench are not at all steep in reality, so it would be the sidewalls of the slit in the electrode having an impact. These sidewalls are metallic, not insulating, and so would not refocus positive ions towards the centre of the slit. The importance of radical generation and reflection may be the dominant one in this case.

4. Conclusions

Many non-ideal profiles can appear when using a patterned electrode to perfom maskless deposition or etching. We have shown a number of such profiles when depositing using a $SiH_4/H_2/Ar$ gas mixture, or when etching using a mixture of $NF_3/Ar/N_2$. A spreading effect outside the area under the slit is present particularly when etching processes are used. For radical limited processes, these profiles may originate in the gas mixture itself (and the diffusivity of the radicals), as well as the effect of the gas mixture on where the precursors are generated within the slit. Broader profiles are likely due to generation near the base of the slit, encouraging diffusion out of the area underneath. The appearance of trenches on either side of the profile can be due to two process occurring simultaneously (deposition and etching), or when only etching is occurring, due to the generation profile and interactions with the walls of the slit.

5. Acknowledgments

The authors acknowledge the financial support of TotalEnergies and the ANR through the PISTOL Industrial Chair Project (ANR-17-CHIN-0002-01).

6. References

[1] R Léal, B Bruneau, P Bulkin, T Novikova, F Silva; N Habka, and EV Johnson, **Plasma Souces Sci. Tech. 29** (2020) 025023.
[2] K. Ouaras, S Filonovich, B Bruneau, J Wang, M Ghosh, and EV Johnson, **Solar Energy Materials and Solar Cells** 246 (2022) 111927.
[3] L. Bárdoš, H. Baránková, and S. Berg, **Surf. Coatings Technol. 97**,(1997) 723.
[4] L. Bárdoš, **Surf. Coatings Technol. 86–87** (1996), 648–656.
[5] T. J. Dalton J. C. Arnold, H. H. Sawin, S. Swan and D. Corliss **J. Electrochem. Soc. 140** (1993) 2395
[6] J. C. Arnold and H. H. Sawin, **J. Appl. Phys. 70** (1991), 5314.
[7] C. Niikura, N. Itagaki, M. Kondo, Y. Kawai, and A. Matsuda, **Thin Solid Films 457** (2004) 84–89
[8] E.A.G. Hamers, A. Fontcuberta i Morral, C. Niikura, R. Brenot, and P. Roca i Cabarrocas, **J. Appl. Phys. 88** (2000) 3674